

Fig. 3 (c) Stress-strain curve for Be at strain rate  $3.7 \times 10^{-1} \text{ sec}^{-1}$

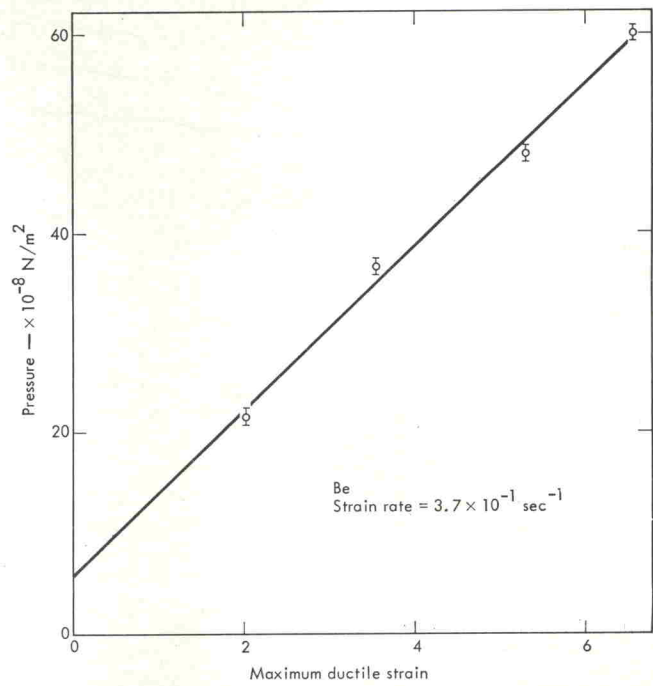


Fig. 5 Maximum ductile shear strain  $\gamma_D$  for the large strain Be data versus pressure

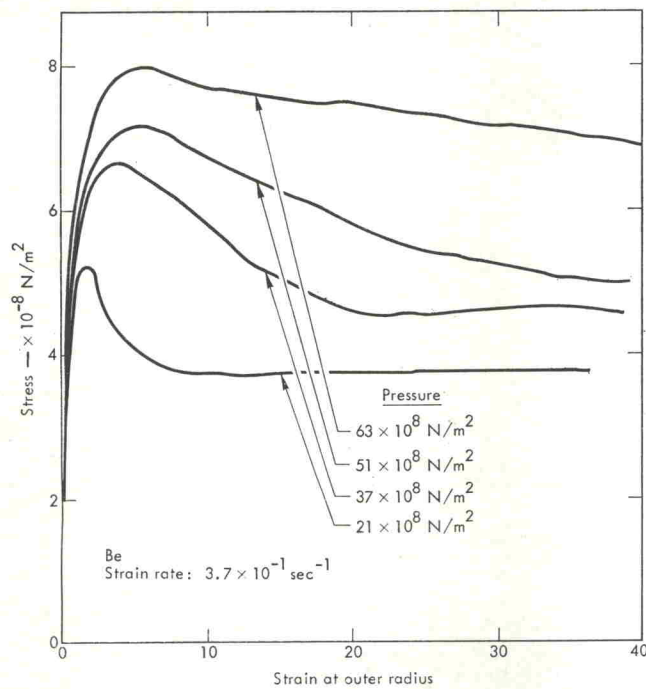


Fig. 4 Large strain Be data taken at  $3.7 \times 10^{-1} \text{ sec}^{-1}$

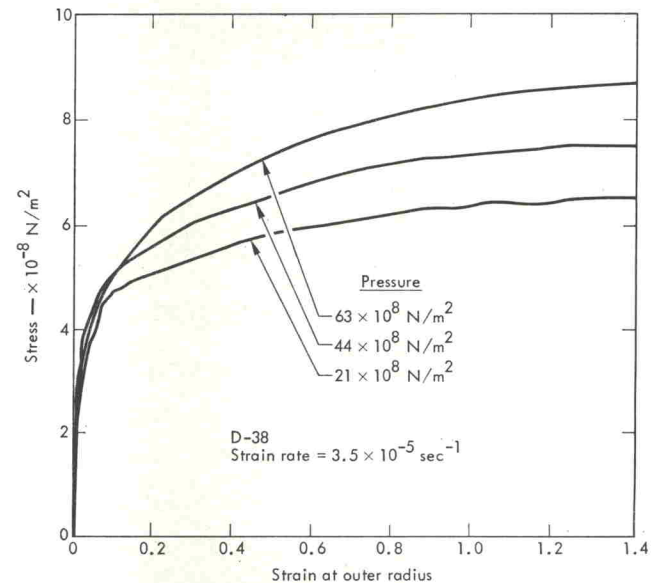


Fig. 6 (a) Stress-strain curve for D-38 at strain rate  $3.5 \times 10^{-5} \text{ sec}^{-1}$

### Experimental Data and Discussion

In Fig. 3 the data for Be are shown. In Fig. 3(a) the data taken at a strain rate of  $3.5 \times 10^{-5} \text{ sec}^{-1}$  are shown for the three pressures (21, 44, and  $63 \times 10^8 \text{ N/m}^2$ ) used in this work. In Figs. 3(b) and 3(c) the data for strain rates of  $3.6 \times 10^{-2} \text{ sec}^{-1}$  and  $3.7 \times 10^{-1} \text{ sec}^{-1}$  are given. As is seen in Fig. 3(c) the curve for a pressure of  $21 \times 10^8 \text{ N/m}^2$  shows a decrease in shear stress for strains larger than 3.8. The curves shown in Fig. 4 were taken at

a strain rate of  $3.7 \times 10^{-1} \text{ sec}^{-1}$  and at pressures of 21, 37, 51,  $63 \times 10^8 \text{ N/m}^2$ . The total strain at the outer radius was increased to approximately 40. These curves show the shear stress increasing with strain up to some given value of strain,  $\gamma_D$ , after which the shear stress decreases with strain. The value of  $\gamma_D$  and the rate of decrease in shear stress are a strong function of pressure. When  $\gamma_D$  is plotted versus pressure as shown in Fig. 5, one can see that  $\gamma_D$  is zero for a pressure of  $6 \times 10^8 \text{ N/m}^2$ . For pressures above  $6 \times 10^8 \text{ N/m}^2$ ,  $\gamma_D$  increases 1.2 for each  $10^9 \text{ N/m}^2$  increase in pressure. For values of strain less than  $\gamma_D$ , the Be samples are believed to be deforming in a ductile mode. At  $\gamma_D$  the Be samples begin to break on a plane parallel to the shear direction. The break is of a more ductile nature at the higher pressures.

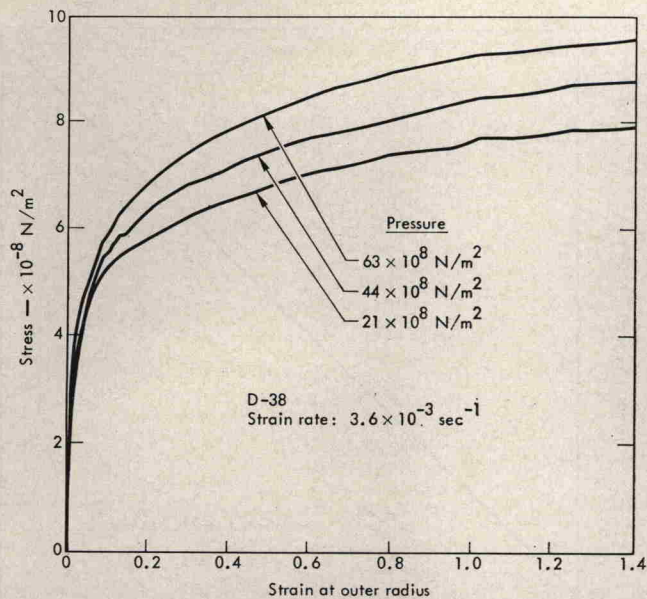


Fig. 6 (b) Stress-strain curve for D-38 at strain rate  $3.6 \times 10^{-3} \text{ sec}^{-1}$

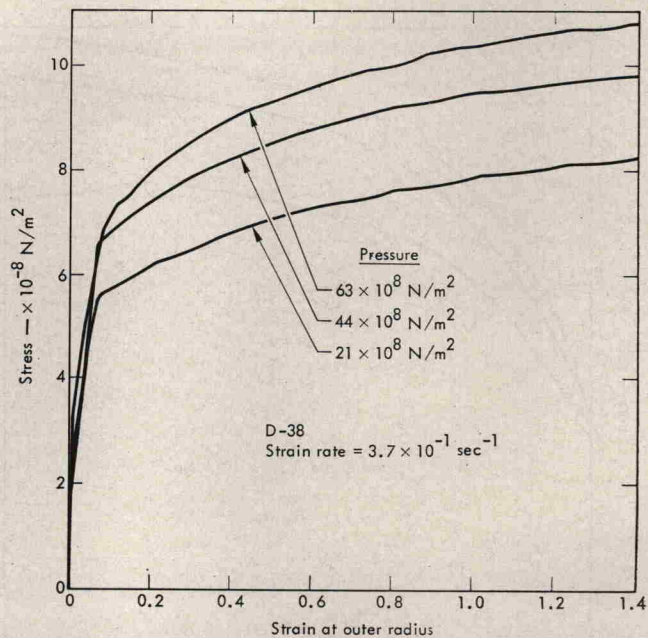


Fig. 6 (c) Stress-strain curve for D-38 at strain rate  $3.7 \times 10^{-1} \text{ sec}^{-1}$

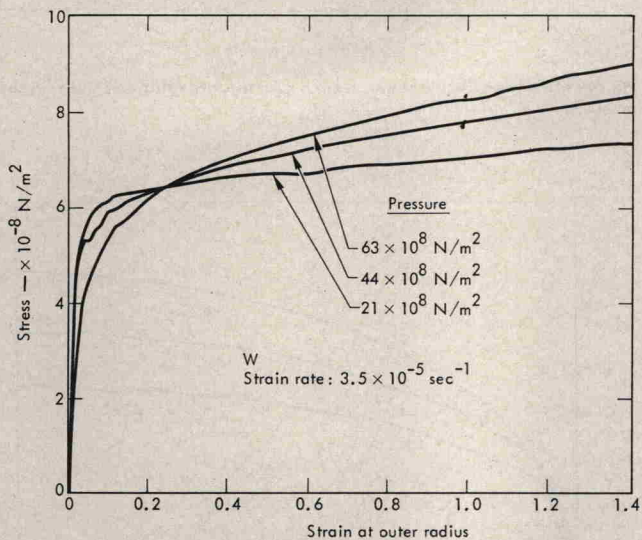


Fig. 7 (a) Stress-strain curve for W at strain rate  $3.5 \times 10^{-5} \text{ sec}^{-1}$

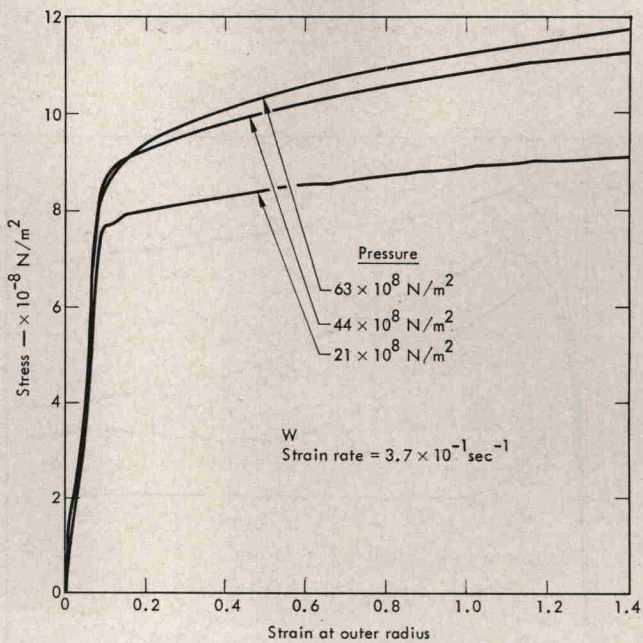


Fig. 7 (c) Stress-strain curve for W at strain rate  $3.7 \times 10^{-1} \text{ sec}^{-1}$

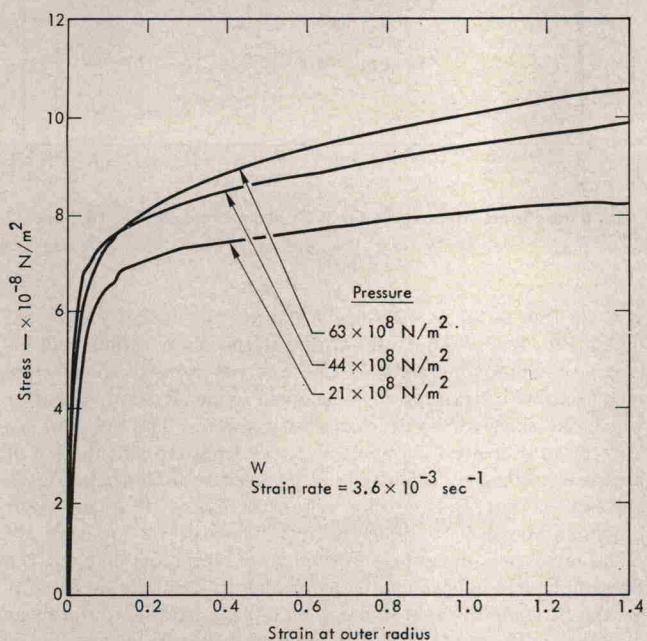


Fig. 7 (b) Stress-strain curve for W at strain rate  $3.6 \times 10^{-3} \text{ sec}^{-1}$

The samples used in these experiments were natural uranium with  $^{235}\text{U}$  depleted, called D-38. The data for D-38 are shown in Figs. 6(a), 6(b), and 6(c) for the three strain rates. For both D-38 and W the low strain data,  $\gamma < 0.05$ , taken at the highest strain rate,  $3.7 \times 10^{-1} \text{ sec}^{-1}$ , cannot be taken too seriously because our experimental technique has not yet been perfected for high strain rate, low strain data.

For tungsten the data, which is still somewhat preliminary, are shown in Figs. 7(a), 7(b), and 7(c). The most interesting of these curves are in Fig. 7(a) for a strain rate of  $3.5 \times 10^{-5} \text{ sec}^{-1}$ . Here for strain less than 0.24 the strength appears to decrease with increasing pressure. If this is really the case and not an experimental idiosyncrasy, a theoretical explanation would be most interesting. For the other strain rates W shows an increase in strength with an increase in pressure for all strains even though there is some scatter in the low strain data.